

## Salt Diffusion and Distribution in Meat Studied by $^{23}\text{Na}$ Nuclear Magnetic Resonance Imaging and Relaxometry

HANNE CHRISTINE BERTRAM,<sup>\*,†</sup> SAMANTHA J. HOLDSWORTH,<sup>§</sup>  
ANDREW K. WHITTAKER,<sup>§</sup> AND HENRIK J. ANDERSEN<sup>†</sup>

Department of Food Science, Danish Institute of Agricultural Sciences, Research Centre Foulum,  
P.O. Box 50, DK-8830 Tjele, Denmark, and Centre for Magnetic Resonance,  
University of Queensland, Queensland 4072, Australia

This study introduces the use of combined  $^{23}\text{Na}$  magnetic resonance imaging (MRI) and  $^{23}\text{Na}$  NMR relaxometry for the study of meat curing. The diffusion of sodium ions into the meat was measured using  $^{23}\text{Na}$  MRI on a 1 kg meat sample brined in 10% w/w NaCl for 3–100 h. Calculations revealed a diffusion coefficient of  $1 \times 10^{-5} \text{ cm}^2/\text{s}$  after 3 h of curing and subsequently decreasing to  $8 \times 10^{-6} \text{ cm}^2/\text{s}$  at longer curing times, suggesting that changes occur in the microscopic structure of the meat during curing. The microscopic mobility and distribution of sodium was measured using  $^{23}\text{Na}$  relaxometry. Two sodium populations were observed, and with increasing length of curing time the relaxation times of these changed, reflecting a salt-induced swelling and increase in myofibrillar pore sizes. Accordingly, the present study demonstrated that pore size and thereby salt-induced swelling in meat can be assessed using  $^{23}\text{Na}$  relaxometry.

**KEYWORDS:** Sodium;  $T_2$  relaxation; curing; salt distribution; muscle; MRI

### INTRODUCTION

A considerable amount of meat is being cured before consumption for preservation and tenderization purposes, and curing by immersion in brine is an essential step in bacon manufacture. However, curing also induces swelling of the meat and allows more water to be bound within the tissue, with a resultant change in the texture of the meat (1, 2). Consequently, understanding the curing process and in particular the diffusion of salt into the meat is of great interest for the meat industry.

Salt diffusion into meat has been studied by measuring the sodium content chemically (3, 4) or by conductometry (5). However, these methods provide no information about the spatial distribution of sodium and, thereby, the migration of sodium into the meat. In contrast, spatial information about the distribution of sodium chloride in dry-cured ham has been measured by computed tomography (CT) (6). However, this method is most suitable for bone tissue and is less accurate for soft tissue, resulting in a poor spatial resolution when muscles are studied. An alternative nondestructive technique containing information about the spatial distribution of salt in meat is  $^{23}\text{Na}$  magnetic resonance imaging (MRI). This was first demonstrated by Renou et al. (7), who studied sodium distribution in processed ham and subsequently used one-dimensional  $^{23}\text{Na}$  MRI to follow the diffusion of sodium ions into pork

during the initial curing process (8). Recently one- and two-dimensional  $^{23}\text{Na}$  MRI has been carried out to study the migration of sodium into pork over 5 days (9). Likewise,  $^{23}\text{Na}$  MRI has been applied on salted fish muscle (10).

$^{23}\text{Na}$  MRI provides information about the salt distribution at the macroscopic level, whereas introduction of  $^{23}\text{Na}$  NMR relaxometry on meat might give information about the sodium ion mobility and distribution at the microscopic level. Presently, numerous  $^1\text{H}$  NMR relaxation applications exist within the meat science area (for a review, see ref 11). In contrast,  $^{23}\text{Na}$  NMR relaxation studies have been very limited (12), due to the lower sensitivity of the  $^{23}\text{Na}$  nucleus in vivo and its short  $T_2$  relaxation time. Despite this, recent years have seen a growing number of papers that have provided direct clinically relevant information for monitoring tissue pathology (13–21). The relaxation behavior of sodium is also complicated by the fact that it has a quadrupole moment ( $I = 3/2$ ), which may result in quadrupolar splitting when in the presence of macromolecules or other environments that induce local field gradients (22). Sodium ions present in such an environment may exhibit two different  $T_2$  relaxation times: a fast and a slow component. However, recently it was demonstrated that the Brownstein–Tarr model is valid for  $^{23}\text{Na}$  relaxation in porous materials and that  $^{23}\text{Na}$  relaxometry can be used to obtain information about pore sizes in such materials (23). A similar concept applied to the  $^{23}\text{Na}$  relaxation in muscle and meat systems would further enhance the information obtained from  $^{23}\text{Na}$  MRI and thereby advance the use of  $^{23}\text{Na}$  MRI as both a diagnostic tool and for applications in food systems.

\* Corresponding author [telephone (+45) 89 99 15 06; fax (+45) 89 99 15 64; e-mail HanneC.Bertram@agrsci.dk].

<sup>†</sup> Danish Institute of Agricultural Sciences.

<sup>§</sup> University of Queensland.

By introducing the combination of  $^{23}\text{Na}$  MRI and  $^{23}\text{Na}$  NMR relaxometry, the aim of the present study was to investigate the diffusion of sodium into meat as well as the effect of sodium concentration and curing time on microscopic sodium distribution and pore sizes in meat.

## EXPERIMENTAL PROCEDURES

**Relaxation Model.** Brownstein and Tarr (24) proposed a model explaining the NMR relaxation in heterogeneous materials such as muscle, which has gained wide acceptance in the interpretation of  $^1\text{H}$  NMR relaxation. According to this model, the relaxation rate is determined by exchange processes between water and macromolecules, where the latter act as relaxation sinks. In the fast diffusion regimen, where the distance to the pore surface is such that the time for the water molecule to diffuse to the surface is shorter than the relaxation time, the relaxation rate is given by

$$\frac{1}{T_2} = \mu \frac{S}{V} \quad (1)$$

where  $\mu$  is the relaxation sink strength,  $S$  is the surface area, and  $V$  is the volume of a pore.

As dissolved ions also move by Brownian motion, Rijniens (23) suggested that the Brownstein–Tarr model potentially also could be applied to describe the relaxation of dissolved ions such as sodium in porous materials. From their investigations, they concluded that  $^{23}\text{Na}$  NMR  $T_2$  relaxometry can be used to monitor pore size distributions. However, the relaxation rate of Na was found to be affected by concentration due to the fact that the bulk relaxation of Na ions is caused by electric field gradients.

When NaCl is added to meat, the myofibril spacing is increased because of increased electrostatic repulsion of the charged protein residues, resulting in a swelling of the meat. Consequently, the relaxation time could be expected to increase in accordance with eq 1. This has already been verified by  $^1\text{H}$  NMR relaxometry (25). In this study, we will determine whether eq 1 also applies to  $^{23}\text{Na}$  relaxation.

**NMR Measurements. Curing Procedure.** Three curing brines based on 10 mM sodium acetate and containing 0.9% (physiologic), 3%, and 6% w/w NaCl, respectively, were made. Subsequently, the pH was adjusted to 5.5 in all curing brines. Twenty-four hours post-mortem, a total of 12 bovine M. supraspinatus were excised, each having a size of approximately  $1 \times 1 \times 2$  cm, and weighed (referred to as weight 1). The samples were placed individually in a container with 20 mL of brine as four replicates of each of the three curing brines. The containers were placed at a temperature of 4 °C, and measurements carried out on days 1, 2, 3, and 6. On each day, one sample from each of the three brines was removed from the salt solution, dabbed, and weighed (referred to as weight 2). From each sample, a subsample of approximately  $1 \times 0.7 \times 0.7$  cm was cut out for NMR measurements. At each point of time, the swelling was determined as the percentage weight gain [ $100 \times (\text{weight } 2 - \text{weight } 1) / \text{weight } 1$ ].

**$^{23}\text{Na}$  NMR Relaxation Measurements.**  $^{23}\text{Na}$  NMR measurements were obtained on a Bruker MSL 300 spectrometer operating at 79.3 MHz for  $^{23}\text{Na}$ . Samples were placed in a glass probe with a diameter of 8 mm.  $^{23}\text{Na}$   $T_2$  relaxation times were measured using the CPMG sequence. The  $T_2$  measurements were performed with a time between subsequent 180° pulses of 400  $\mu\text{s}$ , and the pulse times were 6 and 12  $\mu\text{s}$  for the 90° and 180° pulses, respectively. The amplitude of every second echo in a train of 1024 echoes was acquired with 16 scan repetitions. The repetition time between two succeeding scans was 2 s, which allowed the longitudinal relaxation to return to equilibrium. The measurements were performed at room temperature.

**$^{23}\text{Na}$  Magnetic Resonance Imaging (MRI).**  $^{23}\text{Na}$  MRI of salt diffusion was carried out on a beef muscle of 1 kg. The muscle was placed in a 10% (w/w) NaCl brine at 4 °C. The meat was removed from the brine after 3, 28, 52, 76, and 100 h, and MR images were obtained. After each measurement, the meat was placed back into the brine.

All of the MRI data acquisitions were performed on a 2 T wholebody (Bruker Avance) system equipped with a custom-built dual-tuned

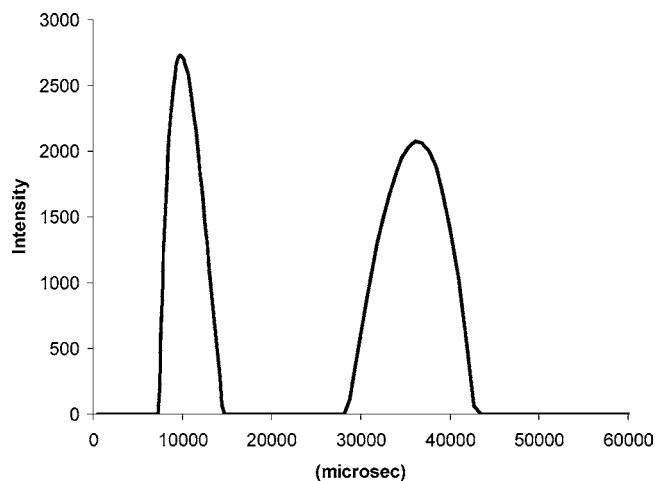


Figure 1.  $T_2$  distribution of sodium in a typical meat sample.

( $^1\text{H}/^{23}\text{Na}$ ) 16 pole birdcage coil operating at 22.6 MHz. Reference proton images were obtained with a standard spin–echo imaging sequence. Prior to imaging, a global shim of the proton resonance across the coil was performed to reduce the main magnetic field inhomogeneity. Sodium images were obtained using a standard spoiled gradient echo sequence with a 2 ms 90° radio frequency pulse, an image slice thickness of 4 cm, a field of view of 24 cm, and a matrix size of  $128 \times 128$ , yielding a pixel resolution of 1.9 mm. An echo time (TE) of 7.6 ms and a repetition time (TR) of 200 ms were used. A total of 256 averages were acquired, resulting in an acquisition time of 1 h and 50 min. An internal reference consisting of 300 mM NaCl was used to scale the images.

## RESULTS

**$^{23}\text{Na}$  NMR Relaxation.** From the obtained  $^{23}\text{Na}$  CPMG relaxation decays, a  $T_2$  distribution was calculated according to the regularization algorithm by Butler et al. (26) and carried out in MatLab version 7.0 using in-house scripts. A representative distribution is shown in Figure 1. Two populations with relaxation times of approximately 10 and 35 ms, respectively, are seen in the  $^{23}\text{Na}$   $T_2$  distribution.

As the  $T_2$  distribution revealed the presence of two relaxation populations, discrete biexponential fitting was performed on the  $^{23}\text{Na}$  CPMG relaxation decays by nonlinear curve fitting by which the relaxation profiles are individually decomposed into a limited number of pure exponential curves (27). The development in the two relaxation time constants, designated the fast ( $T_{2(1)}$ ) and slow ( $T_{2(2)}$ ) components, respectively, and the percentage of the total relaxation that is ascribed to the slower relaxation component ( $T_{2(2)}$ ) as a function of time and NaCl concentration are displayed in Figure 2. Both relaxation components ( $T_{2(1)}$ ,  $T_{2(2)}$ ) increased from day 1 to day 3 and remained relatively constant until day 6 (Figure 2A,B). In addition, the percentage of  $T_{2(2)}$  increased in this same period (Figure 2C), and therefore a concomitant decrease in the proportion of  $T_{2(1)}$  was noted. Figure 3 shows the registered weight gain of the samples. An increase in the degree of weight gain was observed with increasing NaCl concentration, and an increase from day 1 to day 3 followed by little/no weight gain up until day 6 was observed.

**$^{23}\text{Na}$  MRI.** The  $^{23}\text{Na}$  MR images obtained are shown in Figure 4. Clear evidence of progressive diffusion of sodium into the meat is observed with increasing length of curing time, as is also revealed by the sodium intensity profiles in Figure

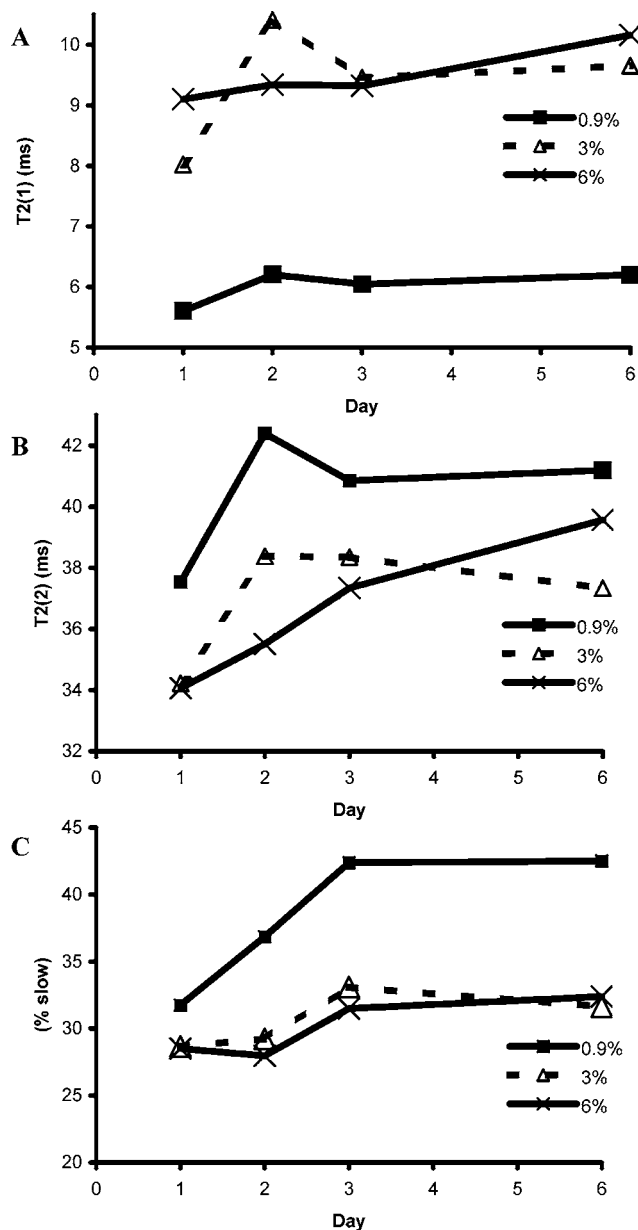


**Figure 2.** Development in  $T_2$  characteristics as a function of curing time and NaCl concentration: (A)  $T_{2(1)}$  shorter time constant; (B)  $T_{2(2)}$  longer time constant; (C)  $T_{2(2)}$  component percentage.

5. To quantify the diffusion of sodium into the meat, the solution to Fick's second law in one dimension (28) was used

$$\frac{C_t}{C_\infty} = 1 - \sum_{n=0}^{\infty} \frac{8}{(2n+1)^2\pi^2} \exp\left[\frac{-D(2n+1)^2\pi^2 t}{4l^2}\right] \quad (2)$$

where  $C$  is the observed concentration of sodium,  $D$  is the diffusion coefficient, and  $l$  is the thickness of the piece. The fit described the data reasonably well and revealed a diffusion coefficient of  $1 \times 10^{-5}$  cm<sup>2</sup>/s after 3 h of curing and a diffusion coefficient of  $8 \times 10^{-6}$  cm<sup>2</sup>/s for the subsequent curing times.

## DISCUSSION

Curing is often used as means of meat preservation in the production of processed meat. Accordingly, the meat industry has a major interest in optimizing curing conditions in relation to final yield and demanded quality characteristics. In the present study <sup>23</sup>Na MRI combined with <sup>23</sup>Na NMR relaxometry enabled

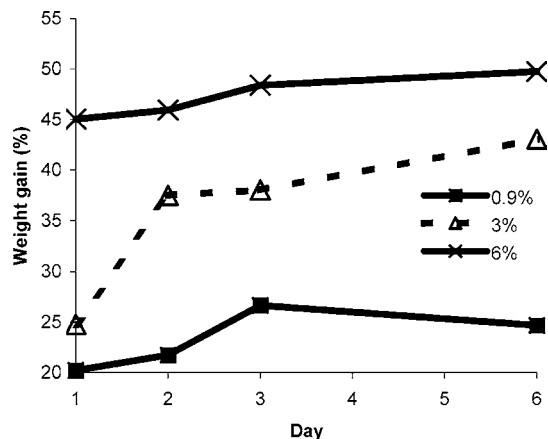


**Figure 3.** Percentage increase in weight for the three sodium concentrations as a function of curing time.

the study of both the diffusion of salt into the meat and the microscopic distribution of the salt within the meat.

<sup>23</sup>Na MR images were obtained from 3 to 100 h of curing and succeeded in displaying a clear progress of diffusion of sodium into the meat. The time course of sodium diffusion during meat curing has also previously been followed using <sup>23</sup>Na NMR imaging; however, this has been either with one-dimensional profiles without any spatial information (8) or on smaller samples (7–9). The diffusion coefficient of sodium was calculated by fitting the data to Fick's second law, which revealed a diffusion coefficient of  $1 \times 10^{-5}$  cm<sup>2</sup>/s after 3 h curing, which subsequently decreased to  $8 \times 10^{-6}$  cm<sup>2</sup>/s at longer curing times. This is in accordance with results by Guiheneuf et al. (8), who investigated the effect of brine sodium concentration and found that the diffusion coefficient decreased exponentially with increasing sodium concentration. Vestergaard et al. (9) also concluded that the diffusion coefficient was changing in the initial stages of the curing process. This could possibly be explained by the sodium-induced solubilization of myosin and simultaneous changes in the microstructure of the meat matrix.

In contrast to <sup>23</sup>Na MRI, <sup>23</sup>Na relaxometry has until now not been attempted to study the salt distribution in cured meat. In the present study the microscopic distribution and mobility of sodium in the meat were studied using <sup>23</sup>Na NMR relaxometry. Distributed fitting analysis revealed the presence of two sodium populations. Two possible explanations exist for this observation: (i) the two observed populations represent two different sizes of pores present in the muscle tissue, or (ii) the two observed populations represent two water fractions in exchange, that is, water close to the surface of pores and "bulk water" in the pores, respectively. We performed triple-quantum filtered imaging of the brine-saturated meat, and this demonstrated that only a small proportion of the signal intensity exhibited triple-quantum coherence. This may at first indicate that the signal of the fast population does not arise from bound sodium due to quadrupolar splitting; however, under some conditions no triple-quantum filtered signal may be observed, despite the presence of bound sodium ions (29). Indeed, Lupu et al. (29) established a bound sodium population exhibiting quadrupolar coherence in liver tissue with  $T_2$  relaxation times of  $\sim 10$ – $15$  ms, on the same order as our fast  $T_2$  component ( $T_{2(1)}$ ). This suggests that the slow  $T_2$  component ( $T_{2(2)}$ ) reflects free sodium ions in the pores, where the quadrupolar interaction is averaged due to rapid molecular motion (extreme narrowing condition), and that the fast component ( $T_{2(1)}$ ) originates from quadrupole-relaxed nuclei

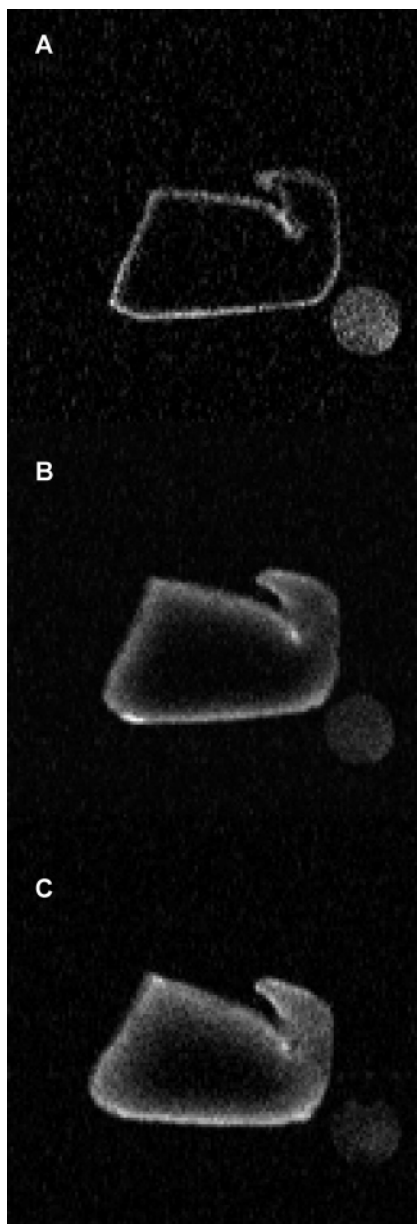


**Figure 4.**  $^{23}\text{Na}$  images showing the progress in sodium interdiffusion: (A) 3 h; (B) 52 h; (C) 100 h. The white circle is a phantom of 300 mM NaCl.

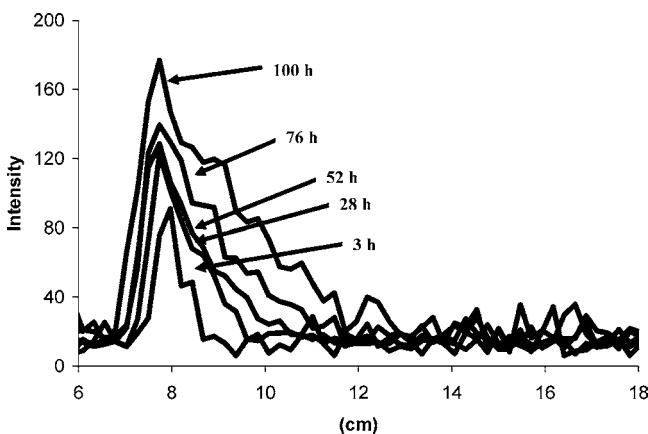


**Figure 5.**  $^{23}\text{Na}$  intensity profiles from 3 to 100 h. The meat sample (1 kg) was brined in 10% w/w NaCl.

from pools where the nuclei are bound to macromolecules that hinder the averaging motions.

When meat is cured, an uptake of water and swelling take place, resulting in larger pore sizes, which was confirmed in the registered weight gain (**Figure 3**). A biexponential fit of the obtained  $T_2$  data, an increase in both  $T_{2(1)}$  and  $T_{2(2)}$  as well as in the proportion of  $T_{2(2)}$ , was observed with increasing length of the curing time. If the two observed populations represent two water fractions in exchange, namely, water close to the surface of pores and bulk water in the pores, the observed tendencies are expected: Swelling will cause more water with a longer diffusional pathway to the surface to be entrapped in the individual pore, and this corresponds to an increased proportion of the  $T_{2(2)}$  component (**Figure 2C**). In addition, ions are further from the relaxation sinks, which is reflected in longer relaxation times of  $T_{2(2)}$  (**Figure 2B**). The observed increase in the  $T_{2(1)}$  relaxation time constant during curing (**Figure 2A**) may be ascribed to a curing-induced change in the constituents/macromolecules binding sodium. This is in agreement with a study on liver, where an increase the relaxation time of the bound population ( $T_{2(1)}$ ) was found during ischemia, which was suggested to reflect changes in the exposure of membrane constituents during tissue deterioration (29). Accordingly, most probably the two sodium populations represent two water fractions in exchange located in the myofibrillar spaces. The present study demonstrates that the characteristics of these  $T_2$  components reflect the degree of salt-induced swelling and pore sizes and that the Brownstein–Tarr model can be applied for  $^{23}\text{Na}$  relaxation in muscle and meat systems. Proton relaxometry on fresh meat exhibits a longer  $T_2$  relaxation component ( $\sim 100$ – $300$  ms) that has been ascribed to extra-myofibrillar water (30). However, proton relaxometry during the curing of meat has revealed that this slow-relaxing population is less evident upon curing (25). Accordingly, it is noticeable that such a population was also not evident in the present  $^{23}\text{Na}$  relaxometry study on cured meat, suggesting that a salt-induced disintegration of the structural features confining intra- and extra-myofibrillar spaces is taking place during curing.

In conclusion, the present study demonstrated that although  $^{23}\text{Na}$  MRI can be used to follow the diffusion of sodium into meat,  $^{23}\text{Na}$  NMR relaxometry is a promising method for characterizing the distribution of sodium structural properties and of cured meat. Further studies combining  $^{23}\text{Na}$  NMR relaxometry with microscopic techniques may strengthen the approach even further in elucidating the structural information contained in the  $^{23}\text{Na}$  NMR data.

#### LITERATURE CITED

- (1) Offer, G.; Trinick, J. On the mechanism of water holding in meat: the swelling and shrinking of myofibrils. *Meat Sci.* **1983**, *8*, 245–281.
- (2) Wilding, P.; Hedges, N.; Lillford, P. J. Salt-induced swelling of meat: the effect of storage time, pH, ion-type and concentration. *Meat Sci.* **1986**, *18*, 53–75.
- (3) Wood, F. W. The diffusion of salt in pork muscle and fat tissue. *J. Sci. Food Agric.* **1966**, *17*, 138–141.
- (4) Rodger, G.; Hastings, R.; Cryne, C.; Bailey, J. Diffusion properties of salt and acetic acid into herring and their subsequent effect on the muscle tissue. *J. Food Sci.* **1984**, *49*, 714–720.
- (5) Djelveh, G.; Gros, J. B. Measurement of effective diffusivities of ionic and non-ionic solutes through beef and pork muscles using a diffusion cell. *Meat Sci.* **1988**, *23*, 11–20.
- (6) Frøystein, T.; Sørheim, O.; Berg, S. A.; Dalen, K. Salt distribution in dry cured hams studied by X-ray tomography. *Fleishwirtschaft* **1989**, *69*, 220–222.
- (7) Renou, J.-P.; Benderbous, S.; Bielicki, G.; Foucat, L.; Donnat, J.-P.  $^{23}\text{Na}$  magnetic resonance imaging: distribution of brine in muscle. *Magn. Reson. Imaging* **1994**, *12*, 131–137.

- (8) Guiheneuf, T.; Gibbs, S. J.; Hall, L. D. Measurement of the inter-diffusion of sodium ions during pork brining by one-dimensional  $^{23}\text{Na}$  magnetic resonance imaging (MRI). *J. Food Eng.* **1997**, *31*, 457–471.
- (9) Vestergaard, C.; Risum, J.; Adler-Nissen, J.  $^{23}\text{Na}$ -MRI quantification of sodium and water mobility in pork during brine curing. *Meat Sci.* **2005**, *69*, 663–672.
- (10) Erikson, U.; Veliyulin, E.; Singstad, T. E.; Aursand, M. Salting and desalting of fresh and frozen-thawed cod (*Gadus morhua*) fillets: a comparative study using Na-23 MRI, low-field H-1 NMR, and physicochemical analytical methods. *J. Food Sci.* **2004**, *69*, E107–E114.
- (11) Bertram, H. C.; Andersen, H. J. NMR applied in meat science. *Annu. Rep. NMR Spectrosc.* **2004**, *53*, 157–202.
- (12) Chang, D. C.; Woessner, D. E. Spin-echo study of  $^{23}\text{Na}$  relaxation in skeletal muscle. Evidence of sodium ions binding inside a biological cell. *J. Magn. Reson. Imaging* **1978**, *30*, 185–195.
- (13) Thulborn, K. R.; Davis, D.; Adams, H.; Gindin, T.; Zhou, J. Quantitative tissue sodium concentration mapping of the growth of focal cerebral tumors with sodium magnetic resonance imaging. *Magn. Reson. Med.* **1999**, *41*, 352–359.
- (14) Boada, F. E.; Christensen, J. D.; Huang-Hellinger, F. R.; Reese, T. G.; Thulborn, K. R. Quantitative in vivo tissue sodium concentration maps: the effects of biexponential relaxation. *Magn. Reson. Med.* **1994**, *32*, 219–223.
- (15) Winkler, S. S.; Thomasson, D. M.; Sherwood, K.; Perman, W. H. Regional  $T_2$  and sodium concentration estimates in the normal brain by sodium-23 MR imaging at 1.5 T. *J. Comput. Assist. Tomogr.* **1989**, *13*, 561–566.
- (16) Winkler, S. S. Sodium-23 magnetic resonance brain imaging. *Neuroradiology* **1990**, *32*, 416–420.
- (17) Bartha, R.; Menon, R. S. Long component time constant of  $^{23}\text{Na}$   $T_2^*$  relaxation in healthy human brain. *Magn. Reson. Med.* **2004**, *52*, 407–410.
- (18) Pabst, T.; Sandstede, J.; Beer, M.; Kenn, W.; Neubauer, S.; Hahn, D. Sodium  $T_2^*$  relaxation times in human heart muscle. *J. Magn. Reson. Imaging* **2002**, *15*, 215–218.
- (19) Bansal, N.; Szczepaniak, L.; Ternullo, D.; Fleckenstein, J. L.; Malloy, C. R. Effect of exercise on  $^{23}\text{Na}$  MRI and relaxation characteristics of the human calf muscle. *J. Magn. Reson. Imaging* **2000**, *11*, 532–538.
- (20) Regatte, R. R.; Kaufman, J. H.; Noyszewski, E. A.; Reddy, R. Sodium and proton MR properties of cartilage during compression. *J. Magn. Reson. Imaging* **1999**, *10*, 961–967.
- (21) Borthakur, A.; Shapiro, E. M.; Beers, J.; Kudchodkar, S.; Kneeland, J. B.; Reddy, R. Sensitivity of MRI to proteoglycan depletion in cartilage: comparison of sodium and proton MRI. *Osteoarthritis Cartilage* **2000**, *8*, 288–293.
- (22) Porion, P.; Al Mukhtar, M.; Meyer, S.; Faugere, A. M.; van der Maarel, J. R. C.; Delville, A. Nematic ordering of suspensions of charged anisotropic colloids detected by  $^{23}\text{Na}$  nuclear magnetic resonance. *J. Phys. Chem. B* **2001**, *105*, 10505–10514.
- (23) Rijniers, L. A.; Magusin, P. C. M. M.; Huinink, H. P.; Pel, L.; Kopinga, K. Sodium NMR relaxation in porous materials. *J. Magn. Reson.* **2004**, *167*, 25–30.
- (24) Brownstein, K. R.; Tarr, C. E. Importance of classical diffusion in NMR studies of water in biological cells. *Phys. Rev. A* **1979**, *19*, 2446–2453.
- (25) Andersen, R. H.; Bertram, H. C.; Andersen, H. J. Curing-induced water mobility and distribution within intra- and extra-myofibrillar spaces of three pork qualities. *Int. J. Food. Sci. Technol.* **2005**, submitted for publication.
- (26) Butler, J. P.; Reeds, J. A.; Dawson, S. V. Estimating solutions of 1<sup>st</sup> kind integral-equations with nonnegative constraints and optimal smoothing. *SIAM J. Numer. Anal.* **1981**, *18*, 381–397.
- (27) Pedersen, H. T.; Bro, R.; Engelsen, S. B. Towards rapid and unique curveresolution of low-field NMR relaxation data: trilinear SLICING versus two-dimensional curve fitting. *J. Magn. Reson.* **2002**, *157*, 141–155.
- (28) Cussler, E. L. *Diffusion: Mass Transfer in Fluid Systems*; Cambridge University Press: Cambridge, U.K., 1997; Chapters 2 and 6.
- (29) Lupu, M.; Ojcius, D.; Perfettini, J. L.; Patry, J.; Dimicoli, J. L.; Mispelter, J. Evidences on sodium ions compartmentalization in biological systems due to pathological states. A non-invasive NMR study. *Biochimie* **2003**, *85*, 849–861.
- (30) Bertram, H. C.; Karlsson, A. H.; Rasmussen, M.; Dønstrup, S.; Petersen, O. D.; Andersen, H. J. Origin of multi-exponential  $T_2$  relaxation in muscle myowater. *J. Agric. Food Chem.* **2001**, *49*, 3092–3100.

---

Received for review May 3, 2005. Revised manuscript received July 11, 2005. Accepted July 25, 2005. The Danish Research Council SJVF is acknowledged for funding the project “Characterization of basic NMR properties in perimortal muscles and meat in relation to physical and metabolic changes” and The Danish Ministry of Food, Agriculture and Fisheries for funding the project “Characterisation of technological and sensory quality in foods” through which the presented data have been obtained and analyzed.

JF051017+